Journal Pre-proofs

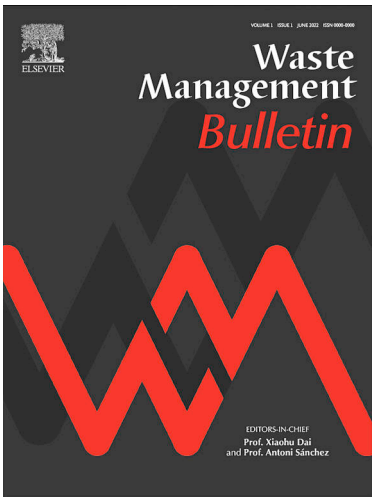

Effect of pyrolysis temperature on the physical and chemical characteristics of pine wood biochar

Berhane Handiso, Timo Pä äkkönen, Benjamin P. Wilson

PII: S2949-7507(24)00098-1
DOI: https://doi.org/10.1016/j.wmb.2024.11.008
Reference: WMB 154

To appear in: *Waste Management Bulletin*

Please cite this article as: Handiso, B., Pä äkkönen, T., Wilson, B.P., Effect of pyrolysis temperature on the physical and chemical characteristics of pine wood biochar, *Waste Management Bulletin* (2024), doi: https://doi.org/10.1016/j.wmb.2024.11.008

Effect of pyrolysis temperature on the physical and chemical characteristics of pine wood biochar

Berhane Handiso[a*], Timo Pääkkönen[b], Benjamin P. Wilson[a,c]

[a]Department of Bioproducts and Biosystems (BIO2), School of Chemical Engineering, Aalto University, FI-00076 Aalto, Finland

[b]Nordic Bioproducts Group Oy; Tietotie 1, 02150 Espoo, Finland

[c]Department of Chemical and Metallurgical Engineering (CMET), School of Chemical Engineering, Aalto University, FI-00076 Aalto, Finland

*Corresponding author

E-mail address: berhane.diso@gmail.com

Department of Bioproducts and Biosystems (BIO2), School of Chemical Engineering, Aalto University, FI-00076 Aalto, Finland

1. Introduction

Biochar is known as a carbon-rich biomaterial that can be used as an environmentally friendly adsorbent material that can be used for the removal of water and wastewater pollutants. For example, Siipola et al., [1] demonstrated the potential use of biochar produced from pine for the removal of polyethylene (PE) microplastics water pollutants

from aqueous environments. Likewise, Wang et al., [2] outlined the use of hardwood and straw biochar for water decontamination, the results of which showed > 95 % retention capacity of polystyrene (PS) microplastics present.

Biomass feedstock for biochar production is abundant, readily available, and economical. Up to 10 - 20 million tonnes of wood waste are generated annually by European countries [3]. Furthermore, the EU mandated set 70 % target retrieval of resources from construction and demolition wastes requires that alternative uses of such materials are needed [3], [4]. In Finland, 58 % of construction and demolition waste is comprised of wood, approximately 40 % of which is currently incinerated for energy recovery [3], [4]. Nevertheless, this wood also has the potential for use in biochar production, which would offer the opportunity for wood waste utilization in a more sustainable manner.

Biochar can be synthesized by several methods including the thermochemical treatment of biomass feedstock using pyrolysis (fast/slow), gasification and hydrothermal carbonization process [5-7]. Of these, the pyrolysis process is a method used to synthesize biochar from biomass in the absence of oxygen gas (O_2), typically at temperatures between (300 - 800 °C) and can be classified as either a slow or fast approach [1], [5], [8-16]. Slow pyrolysis is typically performed at temperatures between (350 - 800 °C) and involves a longer heat residence time of (5 - 10 minutes). Furthermore, slow pyrolysis generally provides a higher yield (30 %) of biochar with higher surface area and porosity. Biochar produced by slow pyrolysis methods is primarily utilized as bio-based absorbent materials to remove water and wastewater pollutants [16]. One study estimates the costs of biochar production via slow pyrolysis as US $ 1000 per tonne of dry feedstock [6]. Another study estimates the cost of biochar production with slow pyrolysis range between US $ 35 - 40 per tonne of biochar excluding transportation costs [5]. In contrast, fast pyrolysis is performed at temperatures between (425 - 550 °C) and typically, has a shorter heat residence time of (~1 or < 2 seconds). This approach results in a lower yield (12 %) of biochar with low surface area/porosity and is typically used to produce bio-oils [1], [5], [6], [16].

Other alternative processes for biochar production include gasification and hydrothermal carbonisation. Gasification only provides low yields (10 %) of biochar and uses a gasification temperature of (≥ 800 °C) in the presence of (O_2). Its heat residence time ranges from (seconds to hours). Gasification is primarily used to produce syngas/synthetic gaseous products [5], [6], [16]. Hydrothermal carbonisation process is a method that converts wet biomass feedstock to pyrolytic liquid and gaseous products at a low-temperature range (180 - 250 °C) in the presence of (O_2) and has heat residence time (several hours to a day). It is believed that biochar produced by hydrothermal carbonization method has a potential use for carbon sequestration [5], [16]. However, depending on the intended application and use, it is also possible to modify the physical and chemical characteristics with several different biochar modification methods, for example, steam, oxygen, carbon dioxide or magnetic activation to improve porosity, pores size, surface area and hydrophobicity [5], [6], [16], [17].

During biochar synthesis, a thermochemical procedure is utilised to convert biomass into carbon-rich material with new/improved properties, consequently the characteristics of a biochar produced are highly dependent on the pyrolysis temperature selected [18]. Other parameters that can influence the biochar properties include pyrolysis operating parameters - like pre-and post-treatment, nitrogen gas (N_2) flow

rate, heating rate, and heat residence time [19]. Nevertheless, among these, pyrolysis temperature is one of the main parameters that influences the overall physicochemical characteristics of any biochar [8-15].

Several studies have previously reported that pyrolysis temperature influence the physical and chemical characteristics of biochar, for instance, biochar's total surface chemistry, surface area, total elemental concentration, yields, pore diameter and degree of porosity. Biochar adsorption property primarily depends on surface chemistry; therefore, it is highly dependent on the surface chemistry and surface area of the biochar [8-10], [12], [14], [15], [20], [21].

Enaime et al., [16] have previously found that biochar produced at high temperatures contains more aromatic functional groups. In addition, further research [5], [22] has suggested that biochar surface chemistry might show hydrophobic, hydrophilic and acidic/basic behaviour depending on different pyrolysis temperatures. Similarly, [5], [16] showed that the hydrophobic nature of biochar surface properties improves as the oxygen and nitrogen content decreases.

Biochar processing temperature can significantly impact the potential application of a biochar [19]. Besides, the use of biochar is substantially dependent on its physical and chemical characteristics [8-10], [12], [14], [15], [20], [21]. Hence, a detailed understanding of the physicochemical variations in biochars that result from different pyrolysis temperatures is essential to be able to tailor their properties. Consequently, this study aims to provide insight and necessary guidance that allows the selection of suitable pyrolysis temperatures to synthesize biochar with the required characteristics for any desired application. The objective of this work is to characterize the biochar derived from pine wood to investigate the influence of processing temperature on the physical and chemical characteristics. This research experimentally evaluates the elemental composition, surface area, density, pore dimeter and volume of produced biochar. In addition, Fourier transfer infrared (FTIR) spectroscopy was utilized to examine the changes in surface functional groups that resulted from the treatment conditions.

Overall, the findings detailed here provides an insight into how biochar physicochemical properties can be affected by different pyrolysis temperatures. Hence, the novelty of this experimental work is that it provides a clear demonstration of the effect of different pyrolysis temperatures used during the slow pyrolysis of pine wood has on the physical and chemical properties of the resultant biochar.

2. Materials and methods

2.1. Materials

Pine wood lumber was provided by Aalto University Wood Workshop, which was cut into squares of 2 × 2 cm^2 area, washed with deionized water and subsequently oven-drying at temperature of 65 °C for 6 hours. Prior to slow pyrolysis, the sample was ground further to reduce the size using a Wiley Mill, (model M02, Arthur H Thomas Co., Pennsylvania, USA).

2.2. Methods

2.2.1. Biochar production

A Nabertherm GmbH, Model RHTH 80 - 300/16, (Nabertherm, Lilienthal, Germany) horizontal tube furnace was used for biochar extraction. The prepared pine wood biomass samples were thoroughly mixed/homogenised prior to subsequent use. When ready, samples were loaded into a ceramic crucible and placed in the middle of a tubular furnace prior to the application of a heating rate of (5 - 10 °C minutes) until the selected pyrolysis temperature was achieved. Biochar was extracted from pine wood by slow pyrolysis at pre-determined temperatures of (300 °C, 500 °C and 800 °C) for 3 hours and (450 °C) for 4 hours with a (N_2) flow rate of 300 L/hour [1]. To examine the effect of pyrolysis heat residence time at 450 °C, the total heat residence time was increased from 3 to 4 hours. After the pyrolysis process was finished, the furnace was turned off to allow the produced biochar to cool down to room temperature while the (N_2) flow maintained until complete. When the tubular furnace was completely cooled, the biochar was removed from the furnace, immediately placed in an airtight glass bottle, and then stored in a desiccator until all the required analyses were completed.

To calculate the yield of biochar, the weight before and after the biochar pyrolysis were recorded. For biochar yield calculation Equation 1 was used [23-25].

$$Biochar\ yield\ (\%) = \frac{Wi}{Wf} \times 100 \qquad \text{Equation 1}$$

Where: W_i = Mass after pyrolysis; W_f = Dry mass (before pyrolysis).

To estimate the moisture content, the dry mass weight of a pine wood biomass sample before and after oven drying at 65 °C for 6 hours was determined. The moisture content estimated using Equation 2 [26], [27].

$$Moisture\ Content\ (\%) = \frac{Wb - Wd\ at\ 65\ °C}{Wb} \times 100 \qquad \text{Equation 2}$$

Where: W_b = Initial weight before dried; W_d = Final weight after dried (at 65 °C for 6 hours).

2.2.2. Surface area and density

Biochar surface area (BET) and pore diameter were analysed by nitrogen gas adsorption-desorption experiments under liquid nitrogen using a Microtrac BELsorp Mini II, (MicrotracBEL, Osaka, Japan). Prior to measurement, samples were pretreated at 100 °C under vacuum for at least 18 hours using a BELPrep VAC II Vacuum Degasser. Data analysis of the adsorption/desorption isotherm to evaluate specific surface area (BET) and pore size was undertaken with BELMaster analysis software (Version 6.4.1.0). In addition, the density and volume of the biochars produced was

measured by helium (He) gas pycnometer, (Ultrapyc 1200e, Quantachrome Instruments, Florida, USA) using a small cell (10 cm^3) and based an average of fifty repetitions.

2.2.3. Elemental analysis

Elemental composition analyses were carried out on the (100 µm) powder biochar grounded by mortar and pestle using Thermo Scientific, Model Flash*Smart* (Thermo Scientific, Waltham, MA, USA) Elemental analyser. The analyser comprised of a double furnace combustion oven set-up with one for CHNS (carbon, hydrogen, nitrogen, sulfur) and the other for O (oxygen). The analysis was performed over a temperature range of (100 - 1100 °C) and the elemental determination of CHNS/O elements was carried out by a thermal conductivity detector.

2.2.4. Fourier transform infrared (FTIR) spectroscopy

Fourier transform infrared spectroscopy (FTIR) analyses were conducted on the (100 µm) powder biochar. The biochar obtained from pyrolysis was finely grounded with mortar and pestle and sieved to fineness size 100 µm using a Retsch sieve, Model 4188 type, (Retsch GmbH, Haan, Germany) and dried at a temperature of 105 °C overnight. A FTIR PerkinElmer, Model Spectrum Two with ATR, (PerkinElmer, Waltham, MA, USA) spectrometer was used combined with Spectrum 10 software, lithium tantalite ($LiTaO_3$) MIR detector and KBr Windows standard optical system. After a rapid scanning of the background, the scan was carried out on each sample and data was taken over a spectral range of 4000 - 500 cm^{-1} based on four repeat scans.

3. Results and discussions

3.1. Yield and Moisture content

Table 1 presents the average moisture contents and yield of biochar in percentage (%). Drying the biomass at the temperature of 65 °C for 6 hours decreases the average moisture content by approx. 8 % of the dry mass. It can be seen from Table 1, the yield (quantity) of biochar decreases from 49.70 %, 24.51 %, 22.49 % and 19.75 % as the pyrolysis temperature increases from (300 °C, 450 °C, 500 °C to 800 °C), respectively. These results correlate with those previously observed by, for example [23], [25], [28], [29].

A possible explanation for the reduction in biochar yield as temperature is increased is either the occurrence of condensation polymerization (i.e. removal of small molecule usually water) or the decomposition or loss of volatile organic compounds – although it could also be a combination of both [24], [25], [28], [30].

At lower pyrolysis temperatures between (300 – 450 °C) there was a significant drop in biochar yield. It is possible that at lower temperatures the macromolecular components (cellulose, hemicellulose, lignin) of the pine wood biomass do not fully convert to biochar [24]. Nevertheless, as the pyrolysis temperature increases between (450 - 800 °C) the decrease in biochar yield was small, which indicates that as the temperature is increased stable carbonaceous content is formed [10]. This observation can also be partly explained by the fact that due to the removal of moisture and volatile organic compounds at lower temperatures, decomposition of the biomass

macromolecular structure is the main causes of the decline in biochar yield at more elevated temperature levels [13], [14], [24], [25], [29].

Decomposition of biomass macromolecule (i.e. cellulose, hemicellulose, lignin) depends on the level of thermal temperatures applied [7]. For example, hemicellulose decomposes at lower pyrolysis temperatures between 200 to 315 °C. The decomposition of hemicellulose releases carbon dioxide (CO_2), carbon monoxide (CO), methane (CH_4) and hydrogen (H_2) gases. In addition, other organic compounds such as alkanes, aldehydes, carboxylic acids, ethers, and small amount of water are byproducts of hemicellulose decomposition [5], [14], [24]. Consequently, this may explain the sharply decline in biochar yield at temperatures between (300 - 450 °C). On the other hands, cellulose decomposes at the intermediate pyrolysis temperature from (300 - 380 °C) and this processes mainly results in the formation of biochar [5], [10], [14], [24]. In contrast, lignin decomposition is known to be a gradual process that commences at around 200 °C and can continue up to a temperature of 900 °C [5], [10], [24].

3.2. Surface area (BET), pore volume and density

Surface area (BET) adsorption desorption analysis results are displayed in Figure 1. As can be seen from Figure 1 (b) there is a marked increase in the surface area and a minor rise in the pore volume at elevated temperature (500 °C). The results of the (BET) and density analysis are presented in Table 2. Additionally, Table 2 also highlights that the density of the biochar was found to slightly increases from 1.28 g/cm^3 to 1.39 g/cm^3 when the pyrolysis temperature increases from (300 °C to 500 °C).

Furthermore, the surface area improves from 1.20 m^2/g to 393 m^2/g, and similarly total pore increase from 0.0151 cm^3/g to 0.1972 cm^3/g when the pyrolysis temperature is increased from (300 °C to 500 °C) (see Table 2). In contrast, the mean pore diameter decreases from the macroporous (~50 nm) to mesoporous region (~2 nm) [31] when temperature increased from (300 °C to 500 °C).

The surface area and porosity increases observed at elevated pyrolysis temperatures shows a similar trend to that previously outlined in the literature [23], [24], [29] which suggests that the likely reasons are caused by the release of vaporous organic material and increase of carbonization. Another possible explanation for observed increase in surface area and pore volume could be caused by the dimensions of the phenol and aromatic groups and substitution of the ester and alkyl groups in lignin [24].

3.3. Elemental composition

Table 3 provides data obtained from elemental analysis and it is clear from the results that there is the rapid decrease in the elemental oxygen (O) and hydrogen (H) content when pyrolysis temperature increases. In comparison, the elemental carbon (C) content increases in parallel with increasing in pyrolysis temperature, probably as a result of the intensification in the degree of carbonization at higher pyrolysis temperatures [24], [25]. The observed reduction in (O) and (H) content as a function of pyrolysis temperature may result from the volatility of organic material and/or destruction of relatively weak oxygen and hydrogen bonds present in hemicellulose, cellulose, and lignin at higher temperatures during pyrolysis [24], [25].

From the Table 3, it can be seen that although the elemental nitrogen (N) is relatively minor, it inclines steadily upwards with higher pyrolysis temperatures. Interestingly, this increase in elemental (N) with pyrolysis temperature differ from those previously detailed in literature [24], [25]. While Vijayaraghavan and Balasubramanian [24] found that the elemental (N) content relatively stable at all pyrolysis temperature ranges and Wei et al., [25] reported that (N) content initially increases before being followed by a gradual decrease with increasing pyrolysis temperature. In this study the elemental sulfur (S) content is stable (i.e. zero) for all pyrolysis temperatures investigated a finding that agrees with previous experimental observations [24].

It is noteworthy that Table 3 shows that when the pyrolysis temperature increases the fraction of (H/C), (O/C) and (O + N)/C steadily declines. The decline of the (H/C) ratio reflects an increase in the degree of carbonization, which indicates that the aromaticity of biochar increases strongly with increasing pyrolysis temperature [24], [25]. The declination of the (O/C) fraction at elevated pyrolysis temperatures provides evidence of the reduction of polar content, which can improve the surface hydrophobicity of biochar [24]. It is apparent from the Table 3 that the ratio of (H/O) is initially small and undergoes a marginal increase at higher pyrolysis temperatures.

3.4. Presence of functional group (FTIR)

The interpretation of Fourier transfer infrared (FTIR) results is mainly based on the work of Coates [32] and Nandiyanto et al., [33] with the support of other relevant studies. As shown in Table 4 and Figure 2 (a and b), the FTIR analysis revealed similarities and variations in their functional groups at different pyrolysis temperatures. Although it is possible residence time affect biochar physicochemical properties, based on the (FTIR) analysis results, this study found that increasing holding time of heating (i.e. heat residence time) has less impact.

The absorbance peak at 3339 cm^{-1} in biochar synthesized at (300 °C) and in the raw pine wood (i.e. reference sample) represents the O-H (alcohol, phenol, or carboxylic acid). The peaks at (2919 cm^{-1}), (2896 cm^{-1}), (2895 cm^{-1}) and (2894 cm^{-1}) in biochar (450 °C), (300 °C), (500 °C) and in raw pine wood in respective order represent C-H stretching (alkanes). The peak at 2161 cm^{-1} in the raw pine wood and in biochar (300 and 800 °C) show the existence of –C≡C– stretch (alkynes). Likewise, the peak at 2049 cm^{-1} in the raw pine wood and in biochar (300 °C) show the presence of –C≡C– stretch (alkynes).

C=C/C=C=C stretching (allene) correspond to the absorbance band at 1980 cm^{-1} in the biochar (500 and 800 °C), and the band at 1979 cm^{-1} in biochar (300 °C). The bands at 1748 cm^{-1} in biochar (800 °C), the band at 1736 cm^{-1} in raw pine wood and the band at 1733 cm^{-1} in biochar (300 °C) correspond to C=O stretching (ester, ketones, aldehydes, carboxylic acid).

C=C is stretching (aromatic ring, conjugated alkene), C=O stretching (conjugated alkene) and/or N-H bending (primary amines) represent the absorbance band at 1604 cm^{-1} in raw pine wood, and the bands at (1596 cm^{-1}), (1586 cm^{-1}), (1584 cm^{-1}) and (1581 cm^{-1}) in biochar synthesized temperature (300 °C), (450 °C), (500 °C) and (800 °C), respectively.

The absorbance bands at 1509 cm^{-1} in biochar synthesized at temperature (300 °C) and the band at 1507 cm^{-1} in raw pine wood corresponds to N-O stretching (nitro compound), C=C/C=C-C aromatic ring stretching and/or N-H bending (primary amines) groups. The band at 1450 cm^{-1} in biochar (300 °C) and the peaks at (1427 and 1373 cm^{-1}) in raw pine wood indicate the presence of C-H bending (alkane) and/or O-H bending (alcohol, phenol, carboxylic acids) within the matrix.

C-O/C-O-C stretching represent the absorbance bands at (1263 and 1024 cm^{-1}) in raw pine wood, the bands at (1264, 1102, 1052 and 1029 cm^{-1}) in biochar (300 °C), the band at 1170 cm^{-1} in biochar (450 °C), the band at 1190 cm^{-1} in biochar (500 °C), and the peaks at (1215 and 1072 cm^{-1}) in biochar synthesized at pyrolysis temperature (800 °C). The bands at (809 and 591 cm^{-1}) in raw pine wood, band at 663 cm^{-1} in biochar (300 °C), bands at (864, 811 and 754 cm^{-1}) in biochar (450 °C) and bands at (863, 811 and 752 cm^{-1}) in biochar (500 °C) assigned to C-H out-of-plane bend (aromatic).

The presence of C-Cl, C-Br, C-I stretching (halo compound) and/or C-H out-of-plane bend (aromatic) are responsible for the band at 559 cm^{-1} in raw pine wood, the peak at 558 cm^{-1} in biochar (300 °C), the peak at 572 cm^{-1} in biochar (450 °C), and the bands at (572, 529, 514, and 502 cm^{-1}) in the biochar synthesized at pyrolysis temperature (800 °C).

4. Conclusions

This study set out to investigate the effect of pyrolysis temperature on the physicochemical properties of biochar derived from pine wood. To accomplish this aim biochar from pine wood biomass was synthesized by a slow pyrolysis method using tubular furnace. For each run at the selected temperatures (300, 500, 800 °C) the tubular furnace heat residence time was selected as 3 hours. In addition, to examine the effect of pyrolysis heat residence time, the heat residence time was increased to 4 hours at the pyrolysis temperature of 450 °C.

Following synthesis, a comprehensive physical (surface area, pore size, pore volume, density, yield) and chemical (surface functional groups, elemental composition) characterization of the biochar was undertaken using Fourier transfer infrared (FTIR) spectroscopy, elemental analysis, and gas adsorption (BET) analysis techniques.

The elemental analysis results show that as pyrolysis temperature increases, the biochar yield, the elemental concentration of oxygen (O) and hydrogen (H) decreases. In contrast, the elemental concentration of carbon (C) significantly increases with pyrolysis temperature increases. The BET analysis shows that the surface area and pore volume increased, whereas the pore size decreased with the increase in pyrolysis temperature. The FTIR analysis revealed similarities and variations in their functional groups at different pyrolysis temperatures. Through the pyrolysis temperatures in the temperature range between (300 - 800 °C), the absorbance bands were developed and/or diminished. This study found that increasing heat residence time has less impact.

Biochar is a renewable and environmentally friendly biomaterial. Pyrolysis temperature is one of the biochar processing conditions which is determined biochar specific application. The present study demonstrates that the physicochemical properties of biochar are highly dependent on the selected pyrolysis temperature. Controlling the pyrolysis temperature helps designing biochar for specific applications for example

adsorbent material for removal of water and wastewater pollutant. Overall, this study provides important information for biochar producers/manufactures that helps to understand the effect of different pyrolysis temperatures, thereby enabling the possibility to produce tailored biochar with the most suitable physicochemical properties for a specific application.

Acknowledgments

Professor Mark Hughes (Aalto University Department of Bioproducts and Biosystems (BIO2)) is acknowledged for discussions on the initial conceptualization process. Timo Kotilahti for sample wood sawing and Rita Hatakka for technical support and providing chemical data. In additions, RawMatTERS Finland Infrastructure (RAMI), hosted by Aalto University and funded by the Academy of Finland is also acknowledged.

References

[1] Siipola, V., Pflugmacher, S., Romar, H., Wendling, L., Koukkari, P., 2020. Low-cost biochar adsorbents for water purification including microplastics removal. Appl. Sci., 10(3), 788. https://doi.org/10.3390/app10030788

[2] Wang, Z., Sedighi, M., Lea-Langton, A., 2020. Filtration of microplastic spheres by biochar: removal efficiency and immobilisation mechanisms. Water Res, 184, 116165. https://doi.org/10.1016/j.watres.2020.116165

[3] Rautkoski, H., Vähä-Nissi, M., Kataja, K., Gestranius, M., Liukkonen, S., Määttänen, M., Liukkonen, J., Kouko, J., Asikainen, S., 2016. Recycling of contaminated construction and demolition wood waste. Waste Biomass Valori, 7(3), 615-624. https://doi.org/10.1007/s12649-016-9481-9

[4] Liikanen, M., Havukalnen, J., Grönman, K., Horttanalnen, M., 2019. Construction and demolition waste streams from the material recovery point of view: A case study of the south karelia region, Finland. Waste Manag. Environ. IX, 231, 171-181. http://doi.org/10.2495/WM180161

[5] Lehmann, J., Joseph, S., 2015. Biochar for environmental management: science, technology and implementation, second ed. Routledge, London. https://doi.org/10.4324/9780203762264

[6] Inyang, M., Dickenson, E., 2015. The potential role of biochar in the removal of organic and microbial contaminants from potable and reuse water: a review. Chemosphere, 134, 232-240. https://doi.org/10.1016/j.chemosphere.2015.03.072

[7] Pecchi, M. and Baratieri, M., 2019. Coupling anaerobic digestion with gasification, pyrolysis or hydrothermal carbonization: a review. Renew. Sustain. Energy Rev., 105, 462-475. https://doi.org/10.1016/j.rser.2019.02.003

[8] Angın, D., Şensöz, S., 2014. Effect of pyrolysis temperature on chemical and surface properties of biochar of rapeseed (Brassica napus L.). Int. J. Phytoremediation, 16(7-8), 684-693. http://doi.org/10.1080/15226514.2013.856842

[9] Chatterjee, R., Sajjadi, B., Chen, W., Mattern, D., Hammer, N., Raman, V., Dorris, A., 2020. Effect of pyrolysis temperature on physicochemical properties and acoustic-based amination of biochar for efficient CO_2 adsorption. Front. Energy Res., 8, 85. https://doi.org/10.3389/fenrg.2020.00085

[10] Chaves Fernandes, B., Ferreira Mendes, K., Dias Júnior, A., da Silva Caldeira, V., da Silva Teófilo, T., Severo Silva, T., Mendonça, V., de Freitas Souza, M., Valadão Silva, D., 2020. Impact of pyrolysis temperature on the properties of eucalyptus wood-derived biochar. Materials., 13(24), 5841. https://doi.org/10.3390/ma13245841

[11] Hadi, A., Norazlina, A., 2021. The effects of pyrolysis temperature on chemical properties of empty fruit bunch and palm kernel shell biochars. In IOP Conference Series: Earth Environ. Sci. 757(1), 012029. https://doi.org/10.1088/1755-1315/757/1/012029

[12] Rodriguez, J., Lustosa Filho, J., Melo, L., de Assis, I., de Oliveira, T., 2020. Influence of pyrolysis temperature and feedstock on the properties of biochars produced from agricultural and industrial wastes. J. Anal. Appl. Pyrol., 149, 104839. http://doi.org/10.1016/j.jaap.2020.104839

[13] Sun, J., He, F., Pan, Y., Zhang, Z., 2017. Effects of pyrolysis temperature and residence time on physicochemical properties of different biochar types. Acta Agric. Scand.,B Soil Plant Sci, 67(1), 12-22. https://doi.org/10.1080/09064710.2016.1214745

[14] Zhang, X., Zhang, P., Yuan, X., Li, Y., Han, L., 2020. Effect of pyrolysis temperature and correlation analysis on the yield and physicochemical properties of crop residue biochar. Bioresour. Technol., 296, 122318. https://doi.org/10.1016/j.biortech.2019.122318

[15] Zhao, L., Cao, X., Mašek, O., Zimmerman, A., 2013. Heterogeneity of biochar properties as a function of feedstock sources and production temperatures. J. Hazard. Mater., 256, 1-9. https://doi.org/10.1016/j.jhazmat.2013.04.015

[16] Enaime, G., Bacaoui, A., Yaacoubi, A., Lübken, M., 2020. Biochar for wastewater treatment—conversion technologies and applications. Appl. Sci., 10(10), 3492. https://doi.org/10.3390/app10103492

[17] Wang, L., Ok, Y., Tsang, D., Alessi, D., Rinklebe, J., Wang, H., Mašek, O., Hou, R., O'Connor, D., Hou, D., 2020. New trends in biochar pyrolysis and modification strategies: feedstock, pyrolysis conditions, sustainability concerns and implications for soil amendment. Soil Use Manag., 36(3), 358-386. http://doi.org/10.1111/sum.12592

[18] Kloss, S., Zehetner, F., Dellantonio, A., Hamid, R., Ottner, F., Liedtke, V., Schwanninger, M., Gerzabek, M., Soja, G., 2012. Characterization of slow pyrolysis biochars: effects of feedstocks and pyrolysis temperature on biochar properties. J. Environ. Qual., 41(4), 990-1000. https://doi.org/10.2134/jeq2011.0070

[19] Claoston, N., Samsuri, A., Ahmad Husni, M., Mohd Amran, M., 2014. Effects of pyrolysis temperature on the physicochemical properties of empty fruit bunch and

rice husk biochars. Waste Manag. Res., 32(4), 331-339. https://doi.org/10.1177/0734242X14525822

[20] Feola Conz, R., Abbruzzini, T., Andrade, C., Milori, D., Cerri, C., 2017. Effect of pyrolysis temperature and feedstock type on agricultural properties and stability biochars. Agric. Sci., 8(9), 914-933. https://doi.org/10.4236/as.2017.89067

[21] González, M., Romero-Hermoso, L., González, A., Hidalgo, P., Meier, S., Navia, R., Cea, M., 2017. Effects of pyrolysis conditions on physicochemical properties of oat hull derived biochar. BioResources, 12(1), 2040-2057. http://doi.org/10.15376/biores.12.1.2040-2057

[22] Palansooriya, K., Yang, Y., Tsang, Y., Sarkar, B., Hou, D., Cao, X., Meers, E., Rinklebe, J., Kim, K., Ok, Y., 2020. Occurrence of contaminants in drinking water sources and the potential of biochar for water quality improvement: A review. Crit. Rev. Environ. Sci. Technol., 50(6), 549-611. http://doi.org/10.1080/10643389.2019.1629803

[23] Askeland, M., Clarke, B., Paz-Ferreiro, J., 2019. Comparative characterization of biochars produced at three selected pyrolysis temperatures from common woody and herbaceous waste streams. PeerJ, 7, e6784. https://doi.org/10.7717/peerj.6784

[24] Vijayaraghavan, K., Balasubramanian, R., 2021. Application of pinewood waste-derived biochar for the removal of nitrate and phosphate from single and binary solutions. Chemosphere, 278, 130361. https://doi.org/10.1016/j.chemosphere.2021.130361

[25] Wei, S., Zhu, M., Fan, X., Song, J., Li, K., Jia, W., Song, H., 2019. Influence of pyrolysis temperature and feedstock on carbon fractions of biochar produced from pyrolysis of rice straw, pine wood, pig manure and sewage sludge. Chemosphere, 218, 624-631. https://doi.org/10.1016/j.chemosphere.2018.11.177

[26] Enders, A. and Lehmann, J., 2017. Proximate analyses for characterising biochars, in: Biochar: a guide to analytical methods, Singh, B., Camps-Arbestain, M., Lehmann, J. (Eds.), CSIRO Publishing, Boca Raton, pp.199-213.

[27] Poonam, Bharti, S.K. and Kumar, N., 2018. Kinetic study of lead (Pb^{2+}) removal from battery manufacturing wastewater using bagasse biochar as biosorbent. Appl. Water Sci., 8, 1-13. https://doi.org/10.1007/s13201-018-0765-z

[28] Uchimiya, M., Wartelle, L., Klasson, K., Fortier, C., Lima, I., 2011. Influence of pyrolysis temperature on biochar property and function as a heavy metal sorbent in soil. J. Agric. Food Chem., 59(6), 2501-2510. http://doi.org/10.1021/jf104206c

[29] Uroić Štefanko, A., Leszczynska, D., 2020. Impact of biomass source and pyrolysis parameters on physicochemical properties of biochar manufactured for innovative applications. Front. Energy Res., 8, 138. https://doi.org/10.3389/fenrg.2020.00138

[30] Zhang, H., Chen, C., Gray, E.M., Boyd, S., 2017. Effect of feedstock and pyrolysis temperature on properties of biochar governing end use efficacy. Biomass Bioenergy, 105, 136-146. http://doi.org/10.1016/j.biombioe.2017.06.024

[31] Thommes, M., Kaneko, K., Neimark, A., Olivier, J., Rodriguez-Reinoso, F., Rouquerol, J., Sing, K., 2015. Physisorption of gases, with special reference to the evaluation of surface area and pore size distribution (IUPAC Technical Report). Pure Appl. Chem., 87(9-10), 1051-1069. https://doi.org/10.1515/pac-2014-1117

[32] Coates, J., 2006. Interpretation of infrared spectra, a practical approach. Encyclopedia Anal. Chem., 12, 10815-10837. https://doi.org/10.1002/9780470027318.a5606

[33] Nandiyanto, A., Oktiani, R., Ragadhita, R., 2019. How to read and interpret FTIR spectroscope of organic material. Indones. J. Sci. Technol., 4(1), 97-118. http://doi.org/10.17509/ijost.v4i1.15806

[34] Cole, E., Zandvakili, O., Xing, B., Hashemi, M., Herbert, S., Mashayekhi, H., 2019. Dataset on the effect of hardwood biochar on soil gravimetric moisture content and nitrate dynamics at different soil depths with FTIR analysis of fresh and aged biochar [dataset]. Data in Brief, 25, 104073. https://doi.org/10.1016/j.dib.2019.104073

[35] Esteves, B., Velez Marques, A., Domingos, I., Pereira, H., 2013. Chemical changes of heat treated pine and eucalypt wood monitored by FTIR. Maderas. Ciencia y Tecnología, 15(2), 245-258. http://doi.org/10.4067/S0718-221X2013005000020

[36] Gámiz, B., Hall, K., Spokas, K., Cox, L., 2019. Understanding activation effects on low-temperature biochar for optimization of herbicide sorption. Agronomy, 9(10), 588. http://doi.org/10.3390/agronomy9100588

[37] Suárez-Hernández, L., Ardila-A., A.N., Barrera-Zapata, R., 2017. Morphological and physicochemical characterization of biochar produced by gasification of selected forestry species. Revista Facultad de Ingeniería, 26(46), 123-130. http://doi.org/10.19053/01211129.v26.n46.2017.7324

[38] Vahur, S., Kriiska, A., Leito, I., 2011. Investigation of the adhesive residue on the flint insert and the adhesive lump found from the Pulli Early Mesolithic settlement site (Estonia) by micro-ATR-FT-IR spectroscopy. Estonian J. Archaeology, 15(1), 3-17. http://doi.org/10.3176/arch.2011.1.01

[39] Wang, C., Wang, Z., Qin, Y., Yin, X., Huang, A., 2018. Released volatile organic compounds in southern yellow pine before and after heat treatment. Int. J. Environ. Res. Public Health, 15(11), 2579. http://doi.org/10.3390/ijerph15112579

[40] Jiménez, E., Aceña-Heras, S., Frišták, V., Heinze, S., Marschner, B., 2018. The effect of biochar amendments on phenanthrene sorption, desorption, and mineralisation in different soils. PeerJ, 6, e5074. http://doi.org/10.7717/peerj.5074

[41] Liu, Y., He, Z., Uchimiya, M., 2015. Comparison of biochar formation from various agricultural by-products using FTIR spectroscopy. Mod. Appl. Sci., 9(4), 246. http://doi.org/10.5539/mas.v9n4p246

[42] Johnston, C., 2017. Biochar analysis by Fourier-transform infra-red spectroscopy, in: Biochar: a guide to analytical methods, Singh, B., Camps-Arbestain, M., Lehmann, J. (Eds.), CSIRO Publishing, Boca Raton, pp.199-213.

[43] Pattnaik, D., Kumar, S., Bhuyan, S., Mishra, S., 2018. Effect of carbonization temperatures on biochar formation of bamboo leaves. In IOP conference series: Mater. Sci. Eng., 338(1), 012054. https://doi.org/10.1088/1757-899X/338/1/012054

[44] Li, X., Song, Y., Bian, Y., Wang, F., Gu, C., Yang, X., Jiang, X., 2019. Effects of root exudates on the sorption of polycyclic aromatic hydrocarbons onto biochar. Environ. Pollut. Bioavailab., 31(1), 156-165. https://doi.org/10.1080/26395940.2019.1593054

Figure 1. Biochar BET adsorption/desorption isotherms at (a) 300 °C and (b) 500 °C.

Figure 2. FTIR comparison (a) before and (b) after normalization of absorbance data.

Table 1. Moisture content, residence time and yields of biochar.

Table 2. Surface area (BET), total pore, mean pore diameter and density of biochar.

Table 3. Elemental concentration in biochar produces at selected temperatures.

Table 4. Functional groups identified in biochar synthesized at selected temperatures.

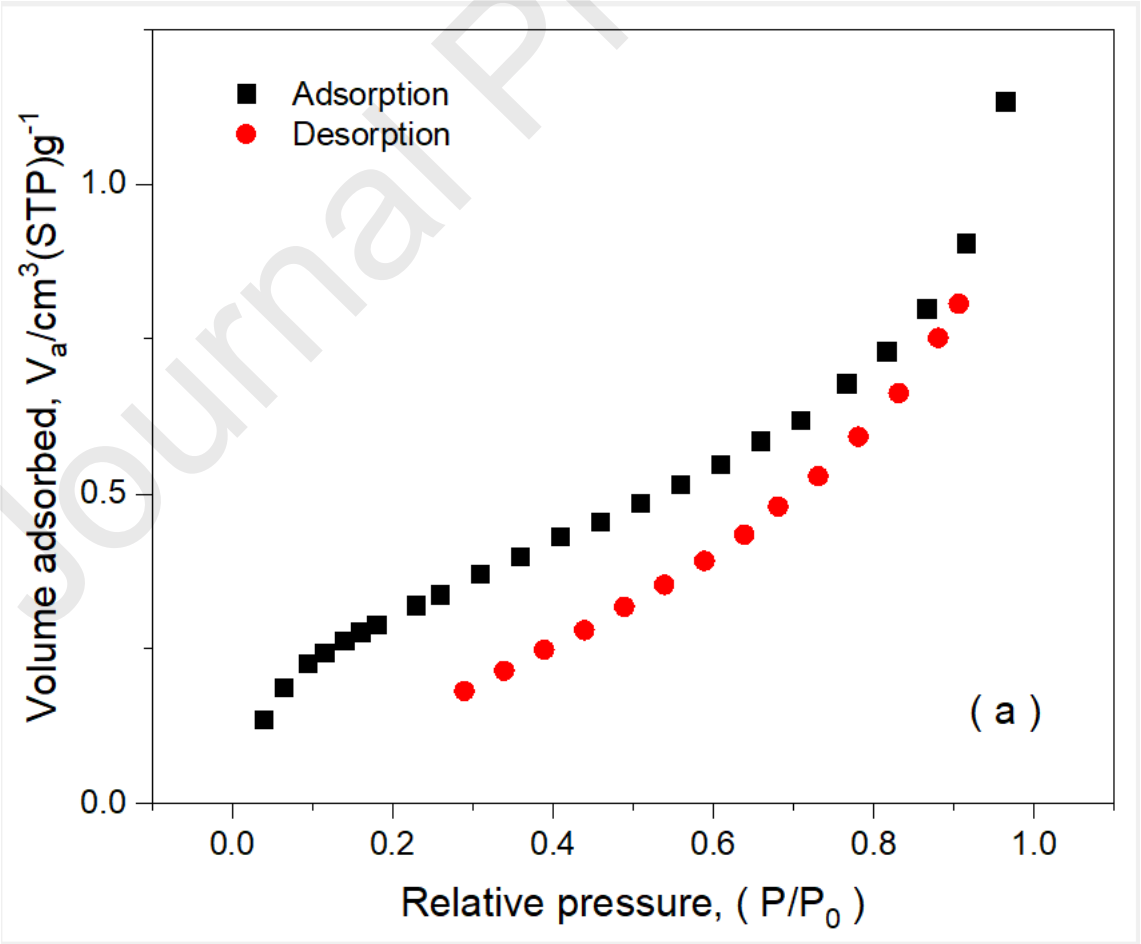

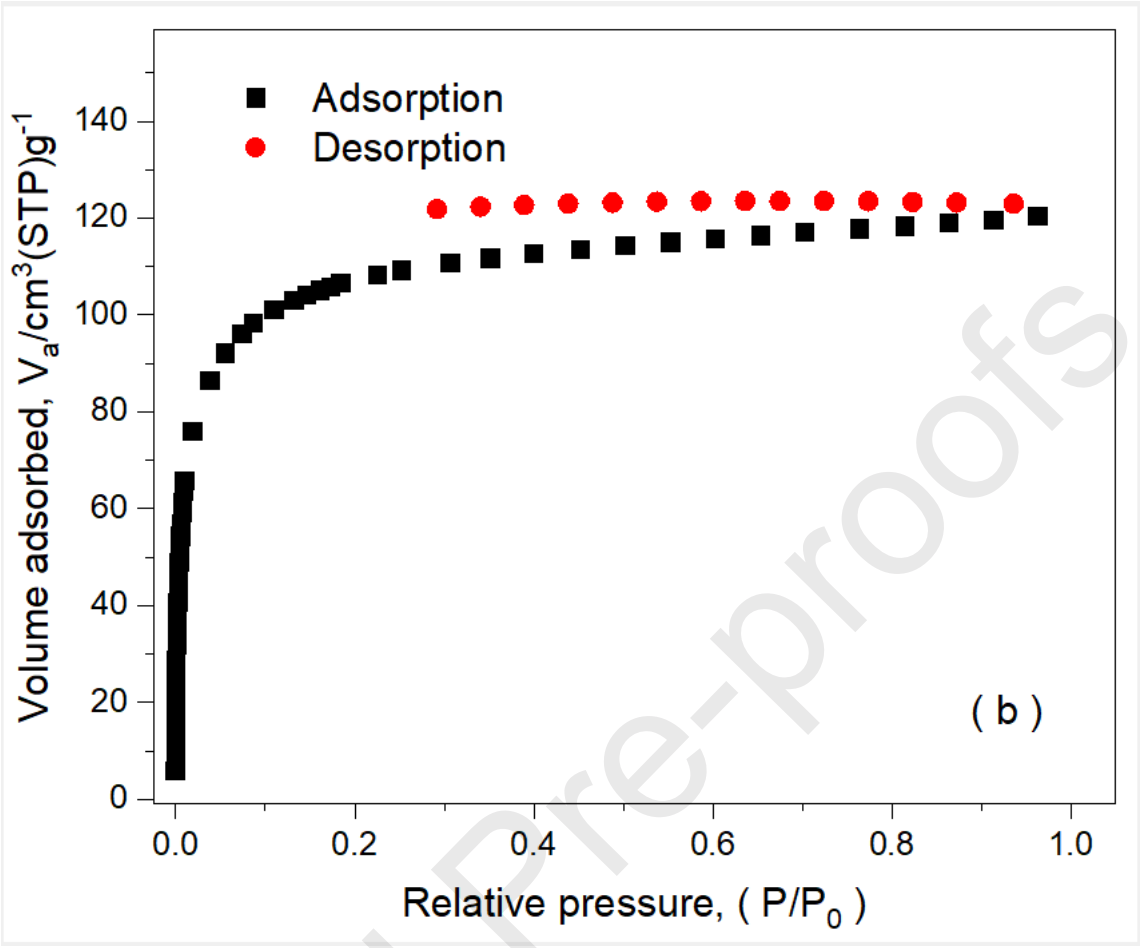

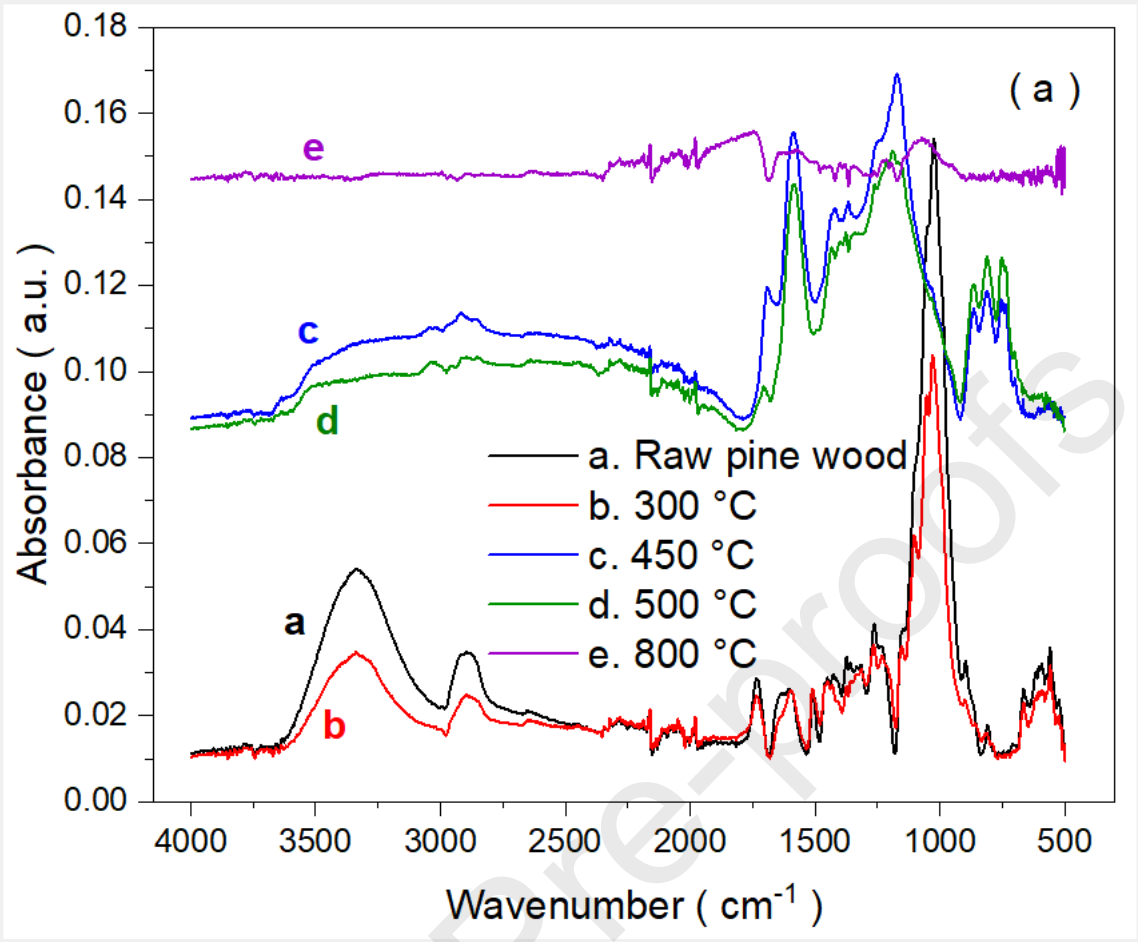

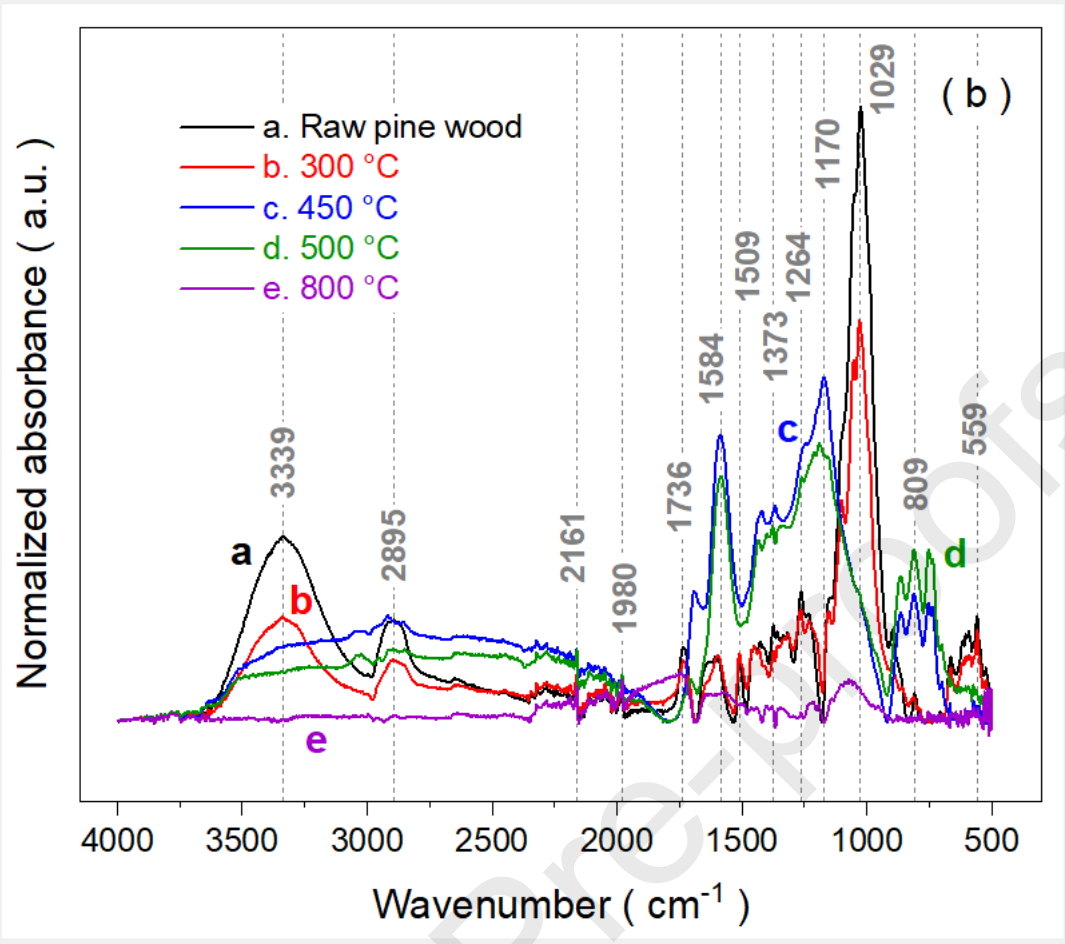

Pyrolysis temperature (°C)	Residence time	Yield (%)	Moisture content (%)
300 °C	3 hours	49.70	8.12
450 °C	4 hours	24.51	8.15
500 °C	3 hours	22.49	8.08
800 °C	3 hours	19.75	8.20

Pyrolysis temperature (°C)	BET surface area (m^2/g)	Total pore (cm^3/g)	Mean pore diameter (nm)	Density (g/cm^3)

300 °C	1.2	0.0151	50.22	1.28
500 °C	393	0.1972	2.01	1.39

	Pyrolysis temperature (°C)		
Element concentration average (%)	450 °C	500 °C	800 °C
Oxygen (O)	12.6506	10.98801	2.504993
Nitrogen (N)	0.079174	0.089235	0.121925
Carbon (C)	82.2771	84.35802	94.45817
Hydrogen (H)	3.423658	3.303805	0.773469
Sulfur (S)	0	0	0
O/C	0.153756	0.130254	0.02652
H/C	0.041611	0.039164	0.008188
H/O	0.270632	0.300674	0.308771
(O+N)/C	0.154718	0.131312	0.027810

Wavenumber (cm^{-1})	Functional groups	References
3339	O–H stretch H–bonded (alcohols, phenols, acids)	[32-39]
2919; 2896; 2895; 2894	C–H stretching (alkanes)	[32, 33, 35-40]

2161; 2049	–C≡C– stretch (alkynes)	[32-34]
1980; 1979	C=C=C stretching (allene); C=C stretching	[32, 33]
1748; 1736; 1733	C=O stretching (ester, ketones, aldehydes, carboxylic acid)	[32, 33, 35, 39, 41]
1604; 1596; 1586; 1584; 1581	C=C stretching (aromatic ring, conjugated alkene); C=O stretching (conjugated alkene); N–H bending (primary amines)	[32-35, 40-43]
1509; 1507	N-O stretching (nitro compound); C=C-C aromatic ring stretching; N–H bending (primary amines)	[32-35, 39, 42, 43]
1450; 1427; 1373	C-H bending (alkane); O-H bending (alcohol, phenol, carboxylic acids)	[32, 33, 35, 38-40, 42]
1264; 1263; 1215; 1190; 1170; 1102; 1072; 1052; 1029; 1024	C-O/C-O-C stretching (alcohols, carboxylic acids, esters, ethers)	[23, 32-35, 38-40]
864; 863; 811; 809; 754; 752; 663; 591	C-H out-of-plane bend (aromatic)	[32-34, 38, 40-43]
572; 559; 558; 529; 514; 502	C-Cl, C-Br, C-I stretching (halo compound); C-H out-of-plane bend (aromatic)	[32, 33, 42, 44]

Graphical abstract

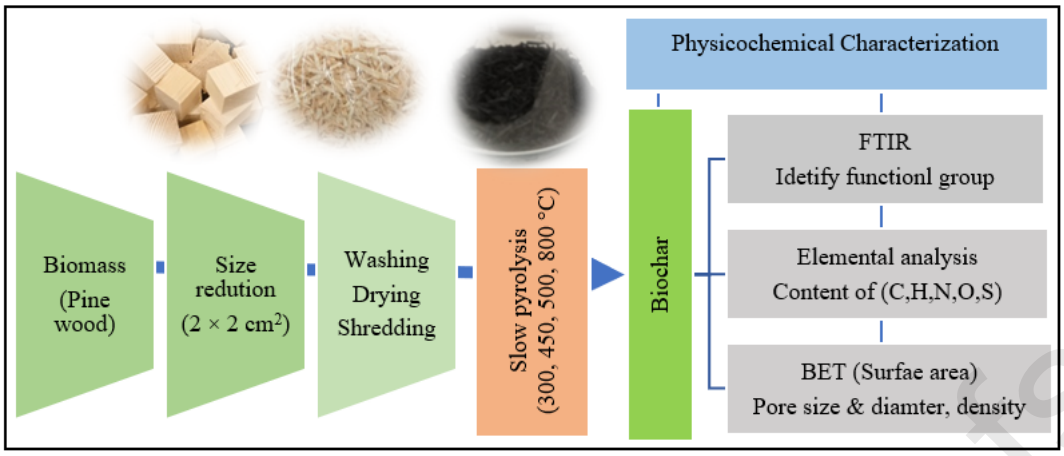

Highlights

- Varying pyrolysis temperatures offered various biochar physicochemical characteristics.
- At higher temperatures, biochar possesses larger carbon and smaller oxygen percentage.
- Increasing pyrolysis temperatures increase surface area and enhance porosity.
- Different pyrolysis temperatures revealed variations of surface functional groups.